NLRP3 Inflammasome Activity is Required for Wound Healing After Burns

Roohi Vinaik[4], **Abdikarim Abdullahi**[4], **Dalia Barayan**[4], **Marc G. Jeschke**[*,1,2,3,4]

[1]Department of Surgery, Division of Plastic Surgery, University of Toronto, Canada

[2]Department of Immunology, University of Toronto, Canada

[3]Ross Tilley Burn Centre, Sunnybrook Health Sciences Centre, Toronto, Canada

[4]Sunnybrook Research Institute, Toronto, Canada

Abstract

Survival of burn patients is contingent on effective wound healing, a complex process that requires coordinated responses of myeloid cells and inflammatory pathways. NLRP3, which serves as a platform for secretion of pro-inflammatory cytokines, is implicated as a central regulator of wound healing. However, its role during the acute dermal and epidermal regeneration in the context of burns is unknown.

Wild-type (WT) and NLRP3$^{-/-}$ mice were exposed to a 30% TBSA scald burn. Gene expression was conducted via RT-PCR. Trichrome staining was used to assess collagen deposition and granulation tissue formation. F4/80 immunostaining compared macrophage infiltration. Flow cytometric analysis was used to characterize skin macrophage distribution and profile.

NLRP3, IL1β and IL18 expression was upregulated in skin after burn, and these changes were non-existent in NLRP3$^{-/-}$. NLRP3$^{-/-}$ had decreased expression of pro-inflammatory cytokines, chemokines, inflammatory markers and growth factors at 3 days ($p<0.05$). NLRP3$^{-/-}$ burn skin demonstrated significantly less macrophage infiltration and higher expression of anti-inflammatory markers Arg1 and Fizz1 ($p<0.05$) compared to WT. Trichrome staining showed decreased collagen deposition compared to WT.

We show that NLRP3 is protective in burn wound healing, primarily through production of inflammatory mediators, macrophage recruitment and polarization to a pro-inflammatory

*Corresponding Author: Marc G. Jeschke, MD, PhD, Director Ross Tilley Burn Centre, Sunnybrook Health Sciences Centre; Division of Plastic Surgery, Department of Surgery, Department of Immunology, University of Toronto; Sunnybrook Research Institute, 2075 Bayview Ave., Rm. D704, Toronto, ON, CANADA, M4N 3M5, Tel: 416-480-6703; Fax: 416-480-6763; marc.jeschke@sunnybrook.ca.

phenotype. Our findings highlight a central role of NLRP3 in wound healing through regulation of inflammation and macrophage polarization after burns.

Keywords

Thermal injury; NLRP3 Inflammasome; Macrophages; Skin; Macrophage Polarization; Glyburide

1.1 INTRODUCTION

Wound healing is a complex process that comprises several phases—inflammation, proliferation, granulation tissue formation, and remodeling. It requires the coordinated response of resident skin cells, soluble factors, and infiltrating inflammatory leukocytes [1]. Principally, inflammatory cells at the site of injury have a complex and critical role in cutaneous healing. However, the benefit of these inflammatory cells and in general, inflammation, is a controversial topic. Prolonged inflammation leads to the formation of chronic wounds and hyperproliferative conditions such as hypertrophic scars or keloids [1,2]. Thus, while acute inflammation may be beneficial, chronic inflammation is detrimental to appropriate wound healing.

Emerging evidence suggests the involvement of inflammasomes in both regulating inflammation required for adequate wound closure and in the pathogenesis of a number of conditions, including sepsis and bury injury. Inflammasomes are multiprotein complexes that have a critical role in innate immunity and are activated in response to cellular damage, tissue injury, and infection. In addition to exogenous pathogen-associated molecular patterns (PAMPs), they are capable of recognizing endogenous, non-infectious, damage-associated molecular patterns (DAMPs) [3]. Nucleotide-binding and oligomerization domain, leucine rich repeat and pyrin domain containing 3 (NLRP3) is the most studied inflammasome and is the only member that recognizes DAMPs, which are released after thermal injury [4]. Upon NLRP3 activation, IL1β and IL18 precursors are processed to generate active cytokines, inducing an inflammatory response. This response has been demonstrated in white adipose tissue of burn patients and in murine excisional wounds, suggesting a putative role in burn wounds [5,6].

In the acute inflammatory period, NLRP3 components are expressed by pro-inflammatory macrophages, which are critical for normal cutaneous responses to injury [7]. Macrophages present at the site of injury are comprised of two groups: resident and infiltrating macrophages. Resident macrophages are present at relatively low levels, and depletion of this population does not have a major effect on macrophage-dependent healing [8]. On the contrary, total macrophage depletion impairs neovascularization and granulation tissue formation, indicating the necessity of recruiting circulating monocytes/macrophages to the site of injury [9].

Macrophages can be further phenotypically classified based on their polarization state, which depends on a variety of local factors such as cytokine expression. These macrophages can be polarized to either a pro-inflammatory or an anti-inflammatory subtype. Pro-inflammatory (also known as classically activated) macrophages are usually produced upon

stimulation with LPS or IFNγ. Anti-inflammatory (alternatively activated) macrophages are produced upon stimulation with cytokines such as IL4 or IL10 [10]. Wound healing relies on a complex balance between pro- and anti-inflammatory macrophages. Macrophage populations change from an early pro- to an anti-inflammatory phenotype as healing progresses, and impaired wound healing can be ascribed to dysregulation of macrophage polarization [11]. For example, unregulated pro-inflammatory populations that fail to switch to anti-inflammatory, pro-healing macrophages are a frequent feature of chronic wounds (e.g. diabetic ulcers) [12,13]. Alternatively, exogenous anti-inflammatory macrophage administration in the acute phase delays wound healing in a mouse diabetic wound model [8]. Taken together, evidence indicates that an intricate balance and a tightly regulated polarization transition are necessary for effective wound healing.

To our knowledge, the relationship between NLRP3 inflammasome activation and macrophage recruitment and polarization in skin after burns has not been elucidated yet. While there are currently a limited number of studies investigating NLRP3 in burn wound healing, we previously established that NLRP3 regulates macrophage recruitment to the liver and adipose tissue after thermal injury [14]. Similarly, we propose that NLRP3 regulates macrophage recruitment and polarization at the site of injury (skin), in addition to the production of inflammatory mediators. Since macrophage recruitment and early inflammation are important elements of wound healing, we postulate that NLRP3 has a protective role in burn wounds. Furthermore, inhibition of NLRP3 activation during the acute phase with drugs such as glyburide would impair normal post-burn cutaneous healing responses.

1.2 METHODS

1.2.1 Human Samples

Patients admitted to the Ross Tilley Burn Center at Sunnybrook Hospital (Toronto, Canada) or non-burn patients undergoing elective surgery were consented preoperatively for tissue collection. Approval for our study was obtained from the Research Ethics Board at Sunnybrook Hospital.

1.2.2 Animals and Model

Animal experiments were conducted in accordance and approved by the Sunnybrook Research Institute Animal Care Committee (Toronto, Ontario, Canada). Wild-type C57/B6 (WT) and NLRP3 knockout (NLRP3$^{-/-}$) male mice (8-10 weeks old, n = 5 per group) were purchased from Jackson Laboratories (Bar Harbor, ME) and housed at ambient temperature and cared in accordance with the Guide for the Care and Use of Laboratory Animals. All mice were anesthetized with 2.5% isoflurane and shaved along the dorsal spine region. Ringer's lactate (2-3 mL) was injected subcutaneously in all treatment mice to protect the spine and buprenorphine (0.05-0.1 mg/kg body weight) was injected for pain management. A full-thickness, third degree dorsal scald burn encompassing 15-20% total body surface area (TBSA) and a 15% wound on the ventral surface was induced by immersing the dorsum of the mice in 98°C water for 10 seconds and the ventral region for 2 seconds. Mice were sacrificed at 3 and 7 days post-burn. Sham mice (control) underwent identical experimental

procedures, with the exception of the burn injury. Dorsal skin tissue was harvested upon sacrifice and stored in −80°C until analysis.

1.2.3 Flow Cytometry

Skin was minced and digested with collagenase (Life Technologies) for 45 minutes at 37°C while shaking. The digested cell suspension was filtered and centrifuged at 1800 rpm for 5 minutes. Pelleted cells were resuspended in FACS buffer (HBSS containing 0.5% BSA) and passed through a 40μM strainer (BD Bioscience) to remove large cellular debris. Cells were stained with monoclonal antibodies on ice for 30 minutes. Samples were than washed and analyzed using BD LSR II Special Order System (BD Biosciences, San Jose, CA, USA). Cells were gated on FSC-A and SSC-A, followed by doublet exclusion (FSC-W x FSC-H, SSC-W x SSC-H). The total percentage of monocytes/macrophages was identified using the following flurochrome-conjugated antibodies: anti-CD45 (anti-mouse PE-Cyanine7, eBioscience), anti-CD11b (anti-mouse Alexa APC-eFluor® 780, eBioscience), and anti-F4/80 (anti-mouse FITC, eBioscience). Anti-inflammatory macrophages were identified using an anti-CD206 antibody (anti-mouse PE, BioLegend) in accordance with the manufacturer's flow cytometry protocol. The gating strategy for assessing innate immune cell distributions included leukocytes initially gated based on granularity and CD45 (side scatter x CD45), followed by size (forward scatter). Gated cells were stained for cell surface markers for monocytes and macrophages (CD11b$^+$/F4/80$^+$).

1.2.4 Histology and Immunohistochemistry

Dorsal skin was collected and immediately fixed in 10% formalin and then maintained in 70% ethanol before paraffin embedding. Subsequently, tissues were sectioned and incubated with F4/80 (Abcam, #100790) for skin macrophages or NLRP3 (Abcam, #214185) followed by DAB staining. For macrophage count, three independent samples were imaged at 40X magnification, and F4/80 positive cells were counted twice manually. For Masson's trichrome staining, paraffin-embedded slides were heated for 30 min at 60°C. The slides were then deparaffinized with citrosol, followed by rehydration through 100% × 2, 95%, 70%, and washed in distilled water. Slides were placed in Bouin's solution (26367–01; EMS, Hatfield, PA, USA) for 1 hour at 56°C and washed. Hematoxylin stain (HHS16; Sigma, Saint Louis, MO, USA) and Biebrich scarlet-acid fuchsin solution were applied sequentially for 10 min. After each stain the slides were washed. Next, slides were differentiated in phosphomolybdic–phosphotungstic acid for 15 min, and transferred to aniline blue for 5 min. All slides were washed in distilled water and then differentiated in 1% acetic acid for 2 min. Slides were dehydrated through 95% ethanol and absolute ethanol followed by clearing in citrosol and were mounted with SHUR/Mount xylene-based liquid mounting media (Triangle Biomedical Sciences, Durham, NC, USA). Imaging was performed on a LSM confocal microscope (Zeiss, Germany).

1.2.5 Glyburide Treatment

Glyburide 50 mg/kg (Sigma-Aldrich) was administered intraperitoneally once every 24 hours and continued until sacrifice at 3 and 7 days. The first dose was administered immediately post-burn, and the final dose was administered 1 hour prior to collection of tissue. For the delayed treatment group, glyburide was administered once daily after 3 days

until sacrifice at 7 days after burn. This dose was chosen as it was previously established to be equivalent to the highest human dose [15].

1.2.6   Gene Expression Using RT-PCR

Total RNA isolated from skin tissue was analyzed by quantitative real-time polymerase chain reaction (RT-PCR). RNA was isolated from tissue and cells using TRIzol-chloroform (Life Technologies) with subsequent purification using the RNeasy Kit (Qiagen) according to the manufacturer's instructions. RNA (2μg) was transcribed to cDNA using the high-capacity cDNA reverse transcription kit (Applied Biosystems). RNA was extracted from rodent skin tissue using Trizol (Invitrogen, CA, USA). Reverse transcription were performed with high-capacity cDNA reverse transcription kit (ABI, MA, USA). RT-PCR was performed using the Applied Biosystems Step One Plus Real-Time PCR System. Gene expression was expressed relative to β-actin and was determined using the following formula: $2^{(-\Delta Ct)}$. Due to inter-species variability, values were expressed as a ratio of burn to sham. Primer sequences used are available upon request.

1.2.7   Western Blotting

Protein from human and rodent skin was extracted in RIPA buffer containing phosphatases and proteases inhibitor cocktails (Roche). Protein concentrations were determined by the BCA protein assay kit (Pierce, Mississauga, ON, Canada). Proteins were resolved by SDS-PAGE followed by western blotting using the following antibodies at 1:1000 concentration: Caspase-1 (Cell Signaling, MA), cleaved caspase-1 (Cell Signaling, MA), IL1β (Cell Signaling, MA), cleaved IL1β (Cell Signaling, MA), and GAPDH (Cell Signaling, MA). Species appropriate secondary antibodies conjugated to horseradish peroxidase (BioRad, Mississauga, ON, Canada) were used and proteins visualized by enhanced chemiluminescence using the BioRad ChemiDoc MP Imaging System. Band intensities were detected, normalized and quantified with the ChemiDoc and Image Lab 5.0 software (BioRad Laboratories, Hercules, CA). Antibody concentrations are expressed relative to GAPDH.

1.2.8   Statistical analysis

All data are represented as mean ± SEM. Statistical analysis was performed using student's t-test, one and two-way ANOVA and Mann–Whitney U test to compare groups, where appropriate. All graphs were created using Graphpad Prism 6.0 (San Diego, CA) and analyzed statistically using SPSS 20 (IBM Corp., NY, NY), with significance accepted at $p < 0.05$ (*), $p < 0.01$ (**), $p < 0.001$ (***) and $p < 0.05$ (#), $p < 0.01$ (##), $p < 0.001$ (###), where appropriate. Asterisks refer to a comparison between burn groups and corresponding shams, and hashtags refer to a comparison between NLRP3$^{-/-}$, WT, and treated mice.

1.2.9   Data Availability

The data set generated during and/or analyzed during the current study are available from the corresponding author on reasonable request.

1.3 RESULTS

1.3.1 Increased expression of NLRP3 and its activation byproducts in human and murine skin after burns

First, we asked if NLRP3 is involved in wound healing after a burn. We conducted a time course study of NLRP3 gene expression in human skin from 25 burn patients (17 male, 8 female) with a mean age of 51 ± 3.19 years and an average TBSA of $30.3 \pm 3.29\%$. Our findings revealed an acute (0-2 days) increase after burn compared to normal skin (13.4 vs. 1.15, $p<0.01$) (Figure 1A). IL1β, an NLRP3 activation byproduct, followed a similar pattern (Figure 1A). IL1β expression was higher acutely, 3-6, and up to 7-10 days after burn compared to normal skin (98.9 vs. 1.65, $p<0.05$; 72.3 vs. 1.65, $p<0.05$; 29.5 vs. 1.65, $p<0.01$). IL18, another NLRP3 activation byproduct, similarly demonstrated significantly higher expression compared to WT at 3-6 days post-burn (1.70 vs. 0.43, $p<0.05$). To confirm our gene expression results, we assessed NLRP3 activation by evaluating the ratio of protein expression of cleaved to pro-caspase-1 and cleaved to pro-IL1β. There is a significant increase in the ratio of cleaved to pro-caspase-1 and cleaved to pro-IL1β at 0-2 days compared to normal skin (0.92 vs. 0.33, $p<0.05$; 29.9 vs. 0.11, $p<0.001$), suggestive of NLRP3 activation (Figure 1A, Figure S1A-D, Figure S1F-I). Furthermore, we stained for NLRP3 in skin obtained from patients 0-2 days after burn, demonstrating that NLRP3 expression is present and more prominent in deeper dermal layers (Figure 1C).

Similar to humans, we show here that NLRP3 gene expression is elevated in WT murine skin at 1 and 3 days after burn (23.1 vs. 1.07 at 1 day, $p<0.001$; 6.76 vs. 1.07 at 3 days, $p<0.05$) (Figure 1B). We also assessed gene expression levels of IL1β and IL18. Analogous to NLRP3, IL1β expression is elevated at 1 and 3 days, although levels are relatively unchanged at 7 days after burn potentially due to contribution from NLRP3-independent IL1β activation pathways (11.7 vs. 1.05 at 1 day, $p<0.0001$; 7.29 vs. 1.05 at 3 days, $p<0.05$; 6.99 vs. 1.05 at 7 days, $p<0.05$) [16-18]. IL18 levels are similarly elevated at 1, 3 and 7 days after burn (4.29 vs. 0.59, $p<0.05$; 8.42 vs. 0.59 at 3 days, $p<0.05$; 3.50 vs. 0.59 at 7 days, $p<0.05$). We compare this to NLRP3$^{-/-}$, which demonstrate no changes in gene expression of NLRP3, IL1β, or IL18 after burn (Figure S2A-C). In order to assess for NLRP3 activation, we measured protein levels of cleaved to pro-caspase-1 and cleaved to pro-IL1β. Similar to our human data, we demonstrate an increase in the ratio of cleaved to pro-caspase-1 and cleaved to pro-IL1β early post-burn (1 and 3 days), with no significant difference at 7 days (Figure 1B, Figure S1E, Figure S1J). Immunohistochemistry for NLRP3 in WT and NLRP3$^{-/-}$ murine skin similarly shows positive dermal expression in WT at 3 days compared to shams, NLRP3$^{-/-}$ and WT at 7 days, which is in accordance with our human data (Figure 1D).

These results indicate that NLRP3 expression is elevated acutely after burns in both human and murine skin. NLRP3 inflammasome expression is localized to the deeper dermal layers of the wound bed, indicating a potential role at the site of injury. Mice wounds show very similar expression profiles for NLRP3 and its activation byproducts when compared to humans, thus allowing for a translational comparison. In order to elucidate the role of

NLRP3 in wound healing, we employed an NLRP3$^{-/-}$ murine model for all of our subsequent studies.

1.3.2 Impaired wound healing and macrophage recruitment to NLRP3$^{-/-}$ skin after burns

Next, we utilized an NLRP3$^{-/-}$ model to assess if lack of NLRP3 would compromise wound healing after burn. We compared healing in WT and NLRP3$^{-/-}$ with trichrome staining of excised wounds (Figure 2A-D). When compared NLRP3$^{-/-}$, WT demonstrated greater dermal collagen deposition and keratinization at 3 days after burn, with further improvements at 7 days (Figure 2A, 2C). Conversely, NLRP3$^{-/-}$ exhibited no changes between 3 to 7 days after burn with regards to collagen deposition (Figure 2B, 2D), suggesting that lack of NLRP3 impairs wound healing. These results indicate that NLRP3 is required for adequate wound closure after burns.

We recently showed that lack of NLRP3 results in differential macrophage recruitment to the liver and adipose tissue [14]. Since macrophages are necessary for granulation tissue formation and release of inflammatory cytokines and growth factors after burns, we next assessed macrophage infiltration to the site of injury. Immunostaining with the macrophage marker F4/80 demonstrates significant dermal macrophage infiltration to the wound site by 3 days in WT compared to NLRP3$^{-/-}$, with more pronounced differences at 7 days after burn (Figure 3A,C). Moreover, F4/80 gene expression in skin was greater in WT versus NLRP3$^{-/-}$ at both time points (9.95 vs. 3.05 at 3 days, p<0.05; 9.50 vs. 4.78 at 7 days, p<0.05) (Figure 3B).

Flow cytometry data corroborates our immunostaining and gene expression results, indicating that NLRP3$^{-/-}$ did indeed have a differential response at 3 and 7 days after burn (Figure 3D). At 3 days after injury, WT have increased macrophage recruitment relative to sham (814 vs. 54 cells, p<0.001) that remains elevated even at 7 days (1120 vs. 54 cells, p<0.001). NLRP3$^{-/-}$ also have increased macrophage infiltration at 3 and 7 days, but these values are significantly less than WT (276 vs. 814 cells at 3 days, p<0.01; 470 vs. 1120 cells at 7 days, p<0.001).

Altogether, these results demonstrate impaired macrophage recruitment to the site of injury in mice that lack NLRP3. Macrophages have an important role in local inflammation, granulation tissue formation, and infection control and as such, are integral to wound healing [19]. Furthermore, studies have previously shown that macrophage polarization is influential in wound healing as well [19]. So, we extended our analysis to compare macrophage polarization between WT and NLRP3$^{-/-}$ at the site of injury.

1.3.3 Increased pro-inflammatory macrophages in the skin in WT after burn

As discussed previously, macrophages can be subdivided into classically activated, pro-inflammatory macrophages or alternatively activated, anti-inflammatory macrophages. Previous studies have utilized pro-inflammatory markers including IL6, CCL2 and IL1β, and anti-inflammatory markers such as Arg1, IL10, Fizz1, and CD206, amongst others [20,21]. While pro-inflammatory macrophages predominate during the acute phase after injury, our flow cytometry analysis indicates a greater percentage of anti-inflammatory CD206-positive macrophages in NLRP3$^{-/-}$ at 3 days (71.3% vs. 58.4%, p<0.05) (Figure

3E), with no significant difference in the percentage of CD206-positive macrophages at 7 days.

Based on this, we subsequently assessed differences in anti- and pro-inflammatory marker expression between WT and NLRP3$^{-/-}$ (Figure 3F). At 3 days, WT display greater expression of pro-inflammatory markers IL6 and CCL2 relative to NLRP3$^{-/-}$ (1.68 vs. 0.49, p<0.05; 3.31 vs. 1.09, p<0.01). Conversely, NLRP3$^{-/-}$ have a higher expression of anti-inflammatory markers Arg1 and Fizz1 at 3 days compared to WT (7.47 vs. 1.13, p<0.001; 6.24 vs. 0.096, p<0.05). However, there are no significant differences in marker gene expression between WT and NLRP3$^{-/-}$ at 7 days. This is consistent with our flow cytometry results, which suggests that WT have a greater pro-versus anti-inflammatory distribution at 3 days when compared to NLRP3$^{-/-}$ (Figure 3E). However, since there are differences in macrophage infiltration between WT and NLRP3$^{-/-}$, we compared relative marker expression between 3 and 7 days within each group (WT and NLRP3$^{-/-}$). We show that WT have lower expression of anti- relative to pro-inflammatory markers at 3 days; however, the opposite expression pattern is seen at 7 days. NLRP3$^{-/-}$ on the other hand have a greater expression of anti-inflammatory markers at all time points (Figure S3).

Under normal conditions, macrophage phenotype changes from an initial pro- to an anti-inflammatory profile [2]. Interestingly, transfer with anti-inflammatory macrophages during the first 3 days after wounding impairs healing [8]. This is consistent with our results of impaired wound healing and the early presence of anti-inflammatory macrophages in NLRP3$^{-/-}$, indicated by increased relative expression of the M2 markers Arg1 and Fizz1 and a greater proportion of CD206-positive macrophages.

1.3.4 Decreased expression of pro-inflammatory cytokines, chemokines, and growth factors in NLRP3$^{-/-}$ skin

Macrophage polarization is regulated by local cytokine levels, and studies have established that production of pro-inflammatory cytokines in injured skin has a central role in wound healing. We previously demonstrated that NLRP3 affects expression of other cytokines and immune mediators in addition to IL1β and IL18 [14,22]. Hence, we subsequently compared expression of several pro-inflammatory cytokines, chemokines, and growth factors in WT and NLRP3$^{-/-}$ skin. As determined earlier, IL1β expression is significantly downregulated in NLRP3$^{-/-}$ compared to WT at all time points (Figure S1b). Similarly, IL6 levels in NLRP3$^{-/-}$ are diminished compared to WT at 3 days (0.49 vs. 1.68, p<0.05) (Figure 4A); however, no difference is seen at 7 days. Interestingly, TNFα expression was elevated in NLRP3$^{-/-}$ at all time points (2.42 vs. 0.23 at 3 days, p<0.001; 6.74 vs. 1.52 at 7 days, p<0.05) (Figure 4B).

Next, we measured expression of the inflammatory chemokine, CCL2. Similar to IL6, NLRP3$^{-/-}$ CCL2 expression is significantly lower than WT at 3 and 7 days (1.09 vs. 3.31, p<0.05; 2.64 vs. 9.34, p<0.05) (Figure 4C). Subsequently, we measured s100a8, which serves as an inflammatory marker in several disease states including psoriasis and hypertrophic scars [23,24]. S100a8 expression is upregulated in the epidermis in response to skin injury, and lack of s100a8 impairs keratinocyte migration and proliferation [6]. Here,

s100a8 expression was downregulated in NLRP3$^{-/-}$ at 3 days (3.85 vs. 9.20, p<0.05) with no significant difference at 7 days (Figure 4D).

We subsequently compared levels of the growth factors VEGF, FGF2, and TGFβ between NLRP3$^{-/-}$ and WT (Figure 4E-G). VEGF and FGF contribute to endothelial cell proliferation and angiogenesis, which ultimately facilitates synthesis of a new extracellular matrix (ECM) following injury. This is succeeded by FGF and TGFβ-mediated fibroblast infiltration and conversion to myofibroblasts, collagen deposition and eventually, scar formation [25]. NLRP3$^{-/-}$ have decreased expression of VEGF, FGF2, and TGFβ at 3 days compared to WT (0.63 vs. 1.86, p<0.01; 0.16 vs. 0.95, p<0.01; 0.76 vs. 1.56, p<0.05). These changes persist at 7 days for VEGF and TGFβ (0.58 vs. 1.70, p<0.05; 1.75 vs. 3.10, p<0.01).

Taken together, these results suggest that lack of NLRP3 consistently decreases early expression of critical factors that are interconnected and involved in different wound healing steps. Decreased production of pro-inflammatory cytokines and chemokines impairs keratinocyte migration and proliferation and immune cell chemotaxis, underscoring the significance of post-injury inflammation in wound healing [13]. Immune cell recruitment (e.g. macrophages) is critical for the production of growth factors and collagen deposition, amongst other functions [26]. Here, we demonstrate diminished macrophage infiltration and altered macrophage phenotype in NLRP3$^{-/-}$. Ultimately, these changes culminate in decreased expression of growth factors and poor keratinization and collagen deposition, suggestive of impaired healing in NLRP3$^{-/-}$.

1.3.5 Glyburide treatment during the acute phase impairs wound healing

Glyburide is a clinically approved drug that also functions as an NLRP3 activation inhibitor. After administering the drug in our murine model, we confirmed that NLRP3 activation byproducts IL1β and IL18 in glyburide treated mice showed significantly lower expression when compared to WT mice (Figure S4). In order to determine if inhibiting NLRP3 during the acute phase results in poor wound healing, we compared the effect of a delayed (3-7 days after burn) to a daily glyburide treatment (0-7 days after burn). To compare healing in treated mice to WT, we performed trichrome staining of the excised wounds (Figure 5A-D). We demonstrate minimal dermal collagen deposition at 3 days in treated skin, a feature also seen in NLRP3$^{-/-}$ skin. Additionally, there were no further improvements at 7 days after burn in treated mice, paralleling NLRP3$^{-/-}$. However, delayed treatment mice at 3 days (equivalent to untreated WT) demonstrated greater collagen deposition compared to the treatment group, as expected. Interestingly, skin from the delayed treatment mice at 7 days after burn had greater collagen deposition compared to mice treated since day 0 after burn.

Earlier, we demonstrated that lack of NLRP3 diminishes macrophage recruitment to the site of injury. Flow cytometry results similarly indicate that daily glyburide treatment results in significantly lower macrophage levels compared to WT at 3 days (266 vs. 814 cells, p<0.01) and 7 days (429 vs. 1120 cells, p<0.001) (Figure 5E). However, delayed glyburide results in a similar pattern of macrophage infiltration to WT untreated mice. Moreover, our data indicated a greater percentage of CD206-positive anti-inflammatory macrophages in glyburide treated mice at 3 days compared to WT (84.8% vs. 58.4%, p<0.05) (Figure 5F).

Taken together, these results suggest that glyburide treatment resembles NLRP3$^{-/-}$ in terms of the underlying mechanistic changes. However, the timing of glyburide administration and therefore, NLRP3 inhibition, is critical to wound healing. Inhibition of NLRP3 after the acute phase (delayed glyburide treatment) mimics WT with regards to wound healing and macrophage infiltration. Contrarily, inhibition during the acute phase (daily treatment) resulted in impaired wound healing and macrophage infiltration.

1.3.6 Glyburide treatment impacts expression of pro-inflammatory cytokines, chemokines, and growth factors

Evidence suggests that glyburide also has a host of anti-inflammatory effects, so we subsequently compared other pro-inflammatory cytokines, chemokines, and growth factor levels in glyburide daily treated and delayed treatment mice to WT and NLRP3$^{-/-}$ as discussed previously [27]. Similar to our flow cytometry and immunohistochemical results, we anticipated that expression levels for daily treated mice should mimic NLRP3$^{-/-}$ and delayed treatment should be similar to WT, highlighting the importance of NLRP3 activation during the acute phase. We initially compared expression of the pro-inflammatory cytokines IL6 and TNFα. There is no significant difference between daily treated and NLRP3$^{-/-}$, and IL6 levels in daily treated and NLRP3$^{-/-}$ mice are similarly diminished compared to WT at 3 days (0.16 vs. 1.68, p<0.01; 0.49 vs. 1.68, p<0.05) (Figure 6A). Similarly, there is no significant difference between daily treatment and NLRP3$^{-/-}$ with regards to TNFα, and both have higher expression of TNFα compared to WT at 7 days (6.48 vs. 1.52, p<0.05; 6.74 vs. 1.52, p<0.05); furthermore, they have greater expression compared to delayed treatment (6.48 vs. 1.42, p<0.05; 6.74 vs. 1.42, p<0.05) (Figure 6B).

We subsequently measured expression of CCL2, demonstrating that daily treated groups had similar levels to NLRP3$^{-/-}$. CCL2 levels are significantly lower than WT at 3 (0.96 vs. 3.31, p<0.001 for daily treated; 1.85 vs. 3.31, p<0.01 for NLRP3$^{-/-}$) and 7 days (4.27 vs. 9.34, p<0.05 for daily treated; 2.64 vs. 9.34, p<0.01 for NLRP3$^{-/-}$), with a similar pattern seen in delayed treatment mice (Figure 6C). Successively, we measured s100a8 and demonstrated that it is downregulated in daily treated and NLRP3$^{-/-}$ mice at 3 days compared to WT (3.81 vs. 9.20, p<0.05 for daily treated; 3.85 vs. 9.20, p<0.05 for NLRP3$^{-/-}$) with no difference at 7 days (Figure 6D).

Thereafter, we compared levels of the growth factors VEGF, FGF2, and TGFβ between treated and WT mice (Figure 6E-G). Treated mice have decreased expression of VEGF (0.095 vs. 1.86, p<0.001) and FGF2 (0.074 vs. 0.95, p<0.001) at 3 days compared to WT with notable differences at 7 days for VEGF and TGFβ (0.55 vs. 1.70, p<0.05; 1.42 vs. 3.10, p<0.01). Similar to the aforementioned markers, delayed treatment had a similar expression pattern to WT.

In summary, these results suggest that blocking NLRP3 activation after thermal injury impairs production of critical growth factors and inflammatory mediators. Consequently, there is diminished macrophage infiltration to the site of injury in treated mice, and macrophages present are potentially anti-inflammatory. Ultimately, these alterations did indeed culminate in impaired wound healing, which is consistent with our NLRP3$^{-/-}$ data.

Specifically, we show here that delayed inhibition of NLRP3 after the acute phase does not compromise wound healing, highlighting the cruciality of acute inflammation.

1.4 DISCUSSION

Skin serves as a protection against microbial invasion and thermal dysregulation. Damage to the skin barrier by thermal injury initiates an immediate inflammatory response that is critical for wound healing. This post-burn inflammation is regulated by NLRP3 inflammasome, which is one of the key mediators of inflammation in tissue injury and infection. As we demonstrate in this study, NLRP3 gene expression is upregulated during the post-burn acute phase (1 and 3 days) in murine skin and from 0-2 days in human skin. Gene expression of the inflammatory cytokines IL1β and IL18, which are NLRP3 activation byproducts, is also upregulated at these time points. Additionally, protein expression of cleaved to pro-caspase-1 and cleaved to pro-IL1β also increases at these time points, providing further evidence of NLRP3 activation. Certain changes persist into the second phase of healing (7 days post-burn in mice, 7-10 days for human IL1β and 3-6 days for human IL18), highlighting the overlap between the different stages of wound healing and the pervasive effects of the early inflammatory response. Indeed, we show that lack of NLRP3 and its inflammatory byproducts impairs post-burn healing, indicated by decreased keratinization and collagen deposition at the site of injury.

After generation of an initial inflammatory response, the next stage of healing involves recruiting circulating monocytes to the wound bed, which later differentiate into mature macrophages [28]. Interestingly, we demonstrate that this is dependent on NLRP3 gene status [14]. In mice that lack NLRP3, there is decreased expression of inflammatory mediators and importantly, chemokines such as CCL2. This corresponds with decreased macrophage recruitment to skin 3 days post-burn, which is sustained at 7 days. Conversely, we see increased macrophage recruitment to the site of injury in mice that express the NLRP3 gene, as expected.

As highlighted earlier, macrophages can be either pro-inflammatory or anti-inflammatory. We show here that macrophages in the first 3 days after burn injury demonstrate greater expression of IL6 and CCL2 relative to Arg1 and Fizz1, suggesting a greater distribution of the pro-inflammatory subtype. Interestingly, NLRP3$^{-/-}$ have greater Arg1 and Fizz1 expression at 3 days relative to IL6 and CCL2, which is indicative of a greater distribution of anti-inflammatory macrophages. Although prolonged pro-inflammatory macrophage activation is deleterious and is a potential cause of chronic wounds, macrophage depletion and transfer with anti-inflammatory macrophages within the first 3 days after wounding is not beneficial; rather, it may impair healing in a diabetic mouse model [8]. Our data is consistent with these findings, and NLRP3$^{-/-}$ mice that express more anti-inflammatory macrophages in this phase have impaired wound healing.

Throughout the stages of wound healing, macrophage infiltration and polarization is critical as macrophages enable tissue repair by initiating the release of cytokines and growth factors such as VEGF, FGF2 and TGFβ [29]. These factors in turn stimulate angiogenesis and induce fibroblast and keratinocyte migration into the wound bed when the early

inflammatory period subsides (2-10 days after wounding) [30]. We demonstrate that at 7 days, relative expression of anti-inflammatory markers is greater than pro-inflammatory, potentially suggesting that the macrophages present are wound healing, anti-inflammatory macrophages. This phenotypic switch is coupled with elevated VEGF and TGFβ expression at 7 days, which is not seen in NLRP3$^{-/-}$.

Taken together, these results show that NLRP3 is necessary for macrophage recruitment after injury and for the production of pro-inflammatory cytokines, chemokines and growth factors. These in turn prompt migration of skin cells into the wound bed and activate the proliferative phase of healing, gradually phasing into the anti-inflammatory remodeling phase seen at 2-3 weeks [31]. It follows then that blocking NLRP3 activation with drugs such as glyburide should have wound impairing effects analogous to the NLRP3$^{-/-}$ model. With respect to inflammatory cytokine, chemokine and growth factor production, we show that post-burn glyburide treatment has similar outcomes to knocking out NLRP3. Treated mice also have decreased recruitment of macrophages to the site of injury, with a predominance of anti-inflammatory rather than pro-inflammatory macrophages at 3 days. Furthermore, trichrome staining of excised burn wounds indicates impaired wound healing in glyburide treated mice, evidenced by poor collagen deposition compared to WT even at 7 days post-burn. Interestingly, treating with glyburide after the acute phase (delayed treatment) abrogates these changes and results in similar wound healing, macrophage recruitment, and gene expression profiles to WT mice, highlighting the importance of acute inflammatory changes in post-burn responses.

However, there are some limitations in the present study. Firstly, this is primarily a rodent study, although it has wider clinical applications as well. For example, glyburide may be administered in the clinical setting as a blood glucose regulator in burn patients in addition to patients with type II diabetes. However, it is important to note that although it regulates NLRP3 activation via inhibition of ATP-sensitive K+ channels, glyburide is not specific for NLRP3. Rather, studies have shown that glyburide can inhibit the P2X7 receptor and the ABC transporter ABC1A [32]. Commercially available MCC950 or JC124 are alternative options and are specific NLRP3 inhibitors. While we utilized glyburide due to its translational aspect, further confirmation using NLRP3-specific inhibitors would be of interest. Another important caveat is that while our data demonstrates that early glyburide administration is detrimental, it does not provide evidence that delayed treatment is beneficial *per se.* Rather, delayed treatment has an analogous outcome to WT. Based on the data provided herein, we can currently only conclude that delayed treatment is less detrimental compared to early treatment. We primarily utilized this model as a further indication that acute inflammation is necessary for normal wound healing.

In this study, we establish a link between post-burn inflammation and wound healing. To our knowledge, this is the first study connecting NLRP3 inflammasome, macrophage recruitment and polarization, and wound healing in burns. Here, we highlight the importance of the inflammatory response in promoting post-burn recovery. Specifically, we demonstrate the necessity of acute inflammation, which is activated in response to microbial invasion or tissue injury, versus chronic hyperinflammation. Hyperinflammation is often seen in various conditions such as cancer, diabetes, and burns and is a maladaptive response that contributes

to poor patient outcomes [33]. Extending our murine results to humans, our data suggests that drugs that mitigate inflammation (e.g. glyburide) should not be prescribed during the acute phase. However, regulating inflammation beyond the acute phase is an important therapeutic strategy. Potentially, delayed inhibition could prevent the development of hyperproliferative conditions without compromising wound healing. However, this is speculative, and we cannot exclude the fact that regulating NLRP3 during the acute phase may be necessary in these cases. Therefore, while we postulate that delayed inhibition of inflammation with glyburide may be beneficial in hyperproliferative conditions, early partial NLRP3 inhibition is a potential alternative. Although previous work has shown increased post-burn mortality in NLRP3$^{-/-}$, partial inhibition by heterozygous knockouts or lower doses of glyburide administered throughout the post-burn phase may be beneficial in severe burn models [14]. However, further murine studies investigating partial NLRP3 inhibition and human studies utilizing delayed or low dose glyburide and wound healing outcomes are needed at this point.

Supplementary Material

Refer to Web version on PubMed Central for supplementary material.

Acknowledgements:

1.5 REFERENCES

[1]. Eming SA, Krieg T, & Davidson JM Inflammation in Wound Repair: Molecular and Cellular Mechanisms. Journal of Investigative Dermatology 127: 514–25, 2007. [PubMed: 17299434]

[2]. Yousuf Y & Amini-Nik S The Role of Myeloid Lineage Cells on Skin Healing and Skin Regeneration. Journal of Tissue Science & Engineering 8, 2017.

[3]. Shao B-Z, Zhe-Qi X, Bin-Ze H, & Ding-Feng S NLRP3 inflammasome and its inhibitors: a review. Front Pharmacol 6: 262, 2015. [PubMed: 26594174]

[4]. Zambetti LP, Laudisi F, Licandro G, Ricciardi-Castagnoli P, & Mortellaro A The rhapsody of NLRPs: master players of inflammation…and a lot more. Immunol Res 53: 78–90, 2012. [PubMed: 22427013]

[5]. Stanojcic M et al. Leukocyte Infiltration and Activation of the NLRP3 Inflammasome in White Adipose Tissue Following Thermal Injury. Crit Care Med 42: 1357–64, 2014. [PubMed: 24584061]

[6]. Ito H, Kanbe A, Sakai H, & Seishima M Activation of NLRP3 signalling accelerates skin wound healing. Experimental Dermatology 27: 80–86, 2018. [PubMed: 28887870]

[7]. Weinheimer-Haus EW, Mirza RE., and Koh TJ Nod-Like Receptor Protein-3 Inflammasome Plays and Important Role during Early Stages of Wound Healing. Plos One 10: e0119106, 2015. [PubMed: 25793779]

[8]. Jetten N, Roumans N, Gijbels MJ, et al. Wound Administration of M2-Polarized Macrophages Does Not Improve Murine Cutaneous Healing Responses. PLoS One 9: e102994, 2014. [PubMed: 25068282]

[9]. Mirza R, DiPietro LA, and Koh TJ Selective and specific macrophage ablation is detrimental to wound healing in mice. Am J Patho. 175: 2454–62, 2009.

[10]. Atri C, Guerfali FZ, & Laouini D Role of Human Macrophage Polarization in Inflammation during Infectious Diseases. Int J Mol Sci 19: 1801, 2018.

[11]. Novak ML & Koh TJ Macrophage phenotypes during tissue repair. J Leukoc Biol 93: 875–81, 2013. [PubMed: 23505314]

[12]. Okizaki S et al. Suppressed recruitment of alternatively activated macrophages reduces TGF-b1 and impairs wound healing in streptozotocin-induced diabetic mice. Biomed Pharmacother 70: 317–25, 2015. [PubMed: 25677561]

[13]. Sindrilaru A et al. An unrestrained proinflammatory M1 macrophage population induced by iron impairs wound healing in humans and mice. J Clin Investig 121: 985–97, 2011. [PubMed: 21317534]

[14]. Vinaik R, Stanojcic M, & Jeschke MG NLRP3 Inflammasome Modulates Post-Burn Lipolysis and Hepatic Fat Infiltration via Fatty Acid Synthase. Scientific Reports 8: 15197, 2018. [PubMed: 30315247]

[15]. Koh GCKW et al. Glyburide Reduces Bacterial Dissemination in a Mouse Model of Melioidosis. PLoS One 7: e2500, 2013.

[16]. Satoh T, Kambe N, & Matsue H NLRP3 activation induces ASC-dependent programmed necrotic cell death, which leads to neutrophilic inflammation. Cell Death Dis 4: 644, 2013

[17]. Lukens JR et al. Critical role for inflammasome-independent IL-1β production in osteomyelitis. PNAS 111: 1066–71, 2014. [PubMed: 24395792]

[18]. Gaidt MM et al. Human Monocytes Engage an Alternative Inflammasome Pathway. Immunity 44: 833–46, 2016. [PubMed: 27037191]

[19]. Krzyszczyk P, Schloss R, Palmer A, & Berthiaume F The Role of Macrophages in Acute and Chronic Wound Healing and Interventions to Promote Pro-wound Healing Phenotypes. Front Physiol 9: 419, 2018. [PubMed: 29765329]

[20]. Jablonski KA et al. Novel Markers to Delineate Murine M1 and M2 Macrophages. PLoS One 10: e0145342, 2015. [PubMed: 26699615]

[21]. Liu C et al. Targeting the Shift from M1 to M2 Macrophages in Experimental Autoimmune Encephalomyelitis Mice Treated with Fasudil. PLoS One 8: e54841, 2013. [PubMed: 23418431]

[22]. Artlett CM & Thacker JD Molecular activation of the NLRP3 Inflammasome in fibrosis: common threads linking divergent fibrogenic diseases. Antioxid Redox Signal 22: 1162–75, 2015. [PubMed: 25329971]

[23]. Funes SC, Rios M, Escobar-Vera J, & Kalergis AM Implications of macrophage polarization in autoimmunity. Immunology 154: 186–95, 2018. [PubMed: 29455468]

[24]. Zhong A et al. S100A8 and S100A9 Are Induced by Decreased Hydration in the Epidermis and Promote Fibroblast Activation and Fibrosis in the Dermis. Am J Pathol 186: 109–22, 2016. [PubMed: 26597884]

[25]. Barrientos S, Stojadinovic O, Golinko MS, Brem H, & Tomic-Canic M Growth factors and cytokines in wound healing. Wound Repair Regen 16: 585–601, 2008. [PubMed: 19128254]

[26]. Artlett CM Inflammasomes in wound healing and fibrosis. Journal of Pathology 229: 157–67, 2013. [PubMed: 23023641]

[27]. Wynn TA & Barron L Macrophages: Master Regulators of Inflammation and Fibrosis. Semin Liver Dis 30: 245–57, 2010. [PubMed: 20665377]

[28]. Rodero MP & Khosrotehrani K Skin wound healing modulation by macrophages. Int J Clin Exp Pathol 3: 643–53, 2010. [PubMed: 20830235]

[29]. Ogle ME, Segar CE, Sridhar S, & Botchwey EA Monocytes and macrophages in tissue repair: Implications for immunoregenerative biomaterial design. Exp Biol Med 241: 1084–97, 2016.

[30]. Gurtner GC, Werner S, Barrandon Y, & Longaker MT Wound repair and regeneration. Nature 453: 314–21, 2008. [PubMed: 18480812]

[31]. Wynn TA & Vannella KM Macrophages in Tissue Repair, Regeneration, and Fibrosis. Immunity 44: 450–62, 2016. [PubMed: 26982353]

[32]. Zhang G, Lin X, Zhang S, Xiu H, Pan C, & Cui W A Protective Role of Glibenclamide in Inflammation-Associated Injury. Mediators Inflamm 2017: 3578702, 2017. [PubMed: 28740332]

[33]. Lamkanfi M, Mueller JL, Vitari AC, Misaghi S, Fedorova A, Deshayes K, Lee WP, Hoffman HM, & Dixit VM Glyburide inhibits the Cryopyrin/Nalp3 inflammasome. J Cell Biol; 187(1): 61–70. [PubMed: 19805629]

Brief Commentary

Background: Survival of burns requires effective wound healing, and aberrant healing increases morbidity and mortality. The benefit of inflammatory cells and inflammation in wound healing is debated. NLRP3 inflammasome is a central regulator of this inflammatory response, and NLRP3 activation acutely post-burn is necessary for immune cell chemotaxis.

Translational Significance: Glyburide is an anti-hyperglycemic and an NLRP3 activation blocker. Although acute inflammation is necessary for healing, chronic inflammation and NLRP3 activation contribute to development of hyperproliferative conditions. We demonstrate that early as opposed to delayed glyburide administration impairs healing, highlighting the potential beneficial effects of acute inflammation in normal wound healing after burns.
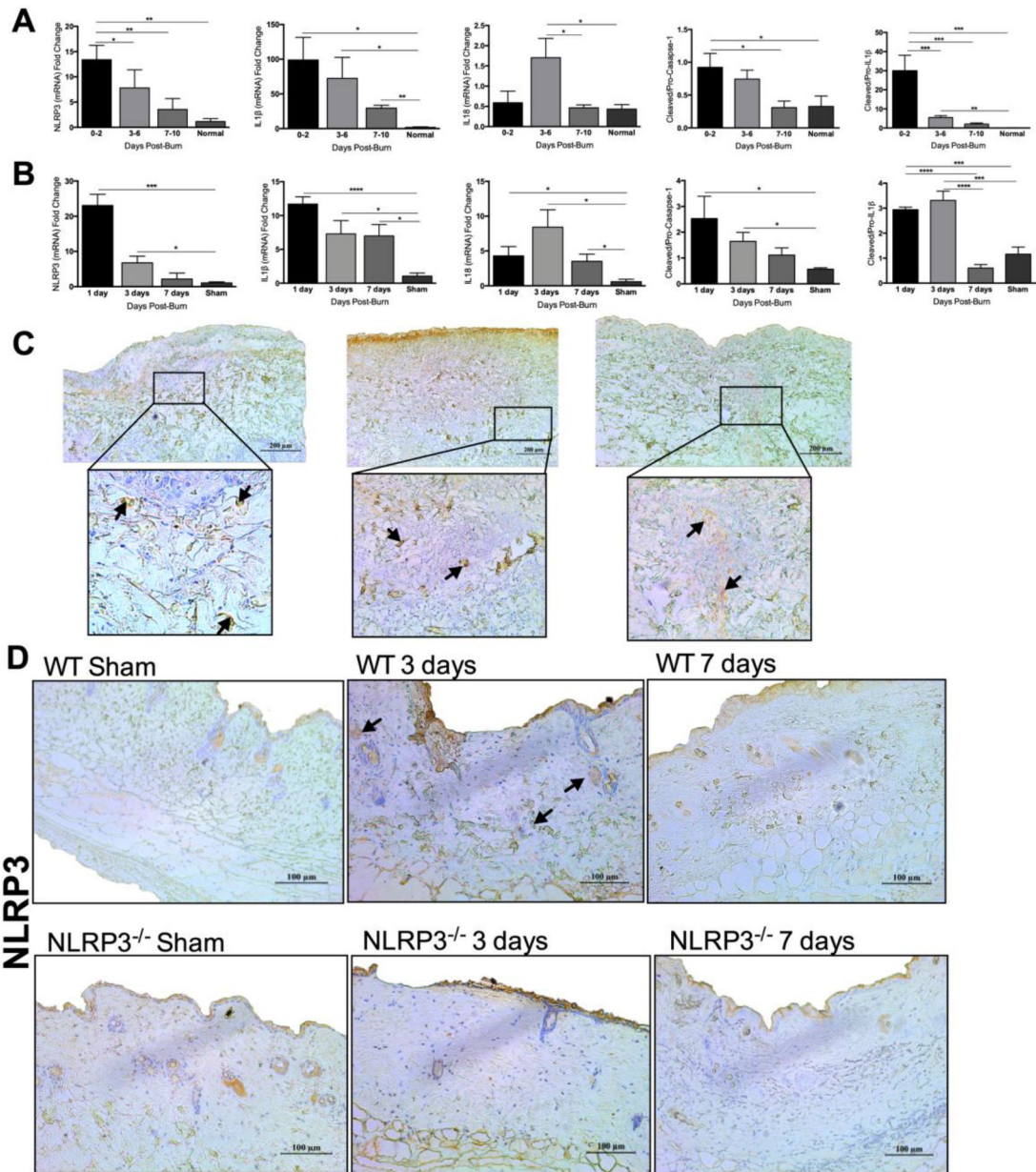
Figure 1.
NLRP3 is upregulated in human and murine skin after burn. (**a**) Time course of gene expression of NLRP3, IL1β and IL18 and protein expression of cleaved to pro-caspase-1 and cleaved to pro-IL1β at 0-10 days after burn compared to normal skin. (**b**) Gene expression of NLRP3, IL1β and IL18 and protein expression of cleaved to pro-caspase-1 and cleaved to pro-IL1β in murine skin after burn. (**c**) Immunohistochemical staining for NLRP3 at 0-2 days post-burn in human burn skin indicates more NLRP3 positive cells in the dermis. (**d**) Staining for NLRP3 at 3 and 7 days after burn in murine skin indicates more NLRP3 positive cells in the dermis of WT at 3 days. Areas of positive staining are marked with an arrow. Values are presented as mean ± standard error. Burn versus normal skin *p < 0.05; **p < 0.01; ***p<0.001.
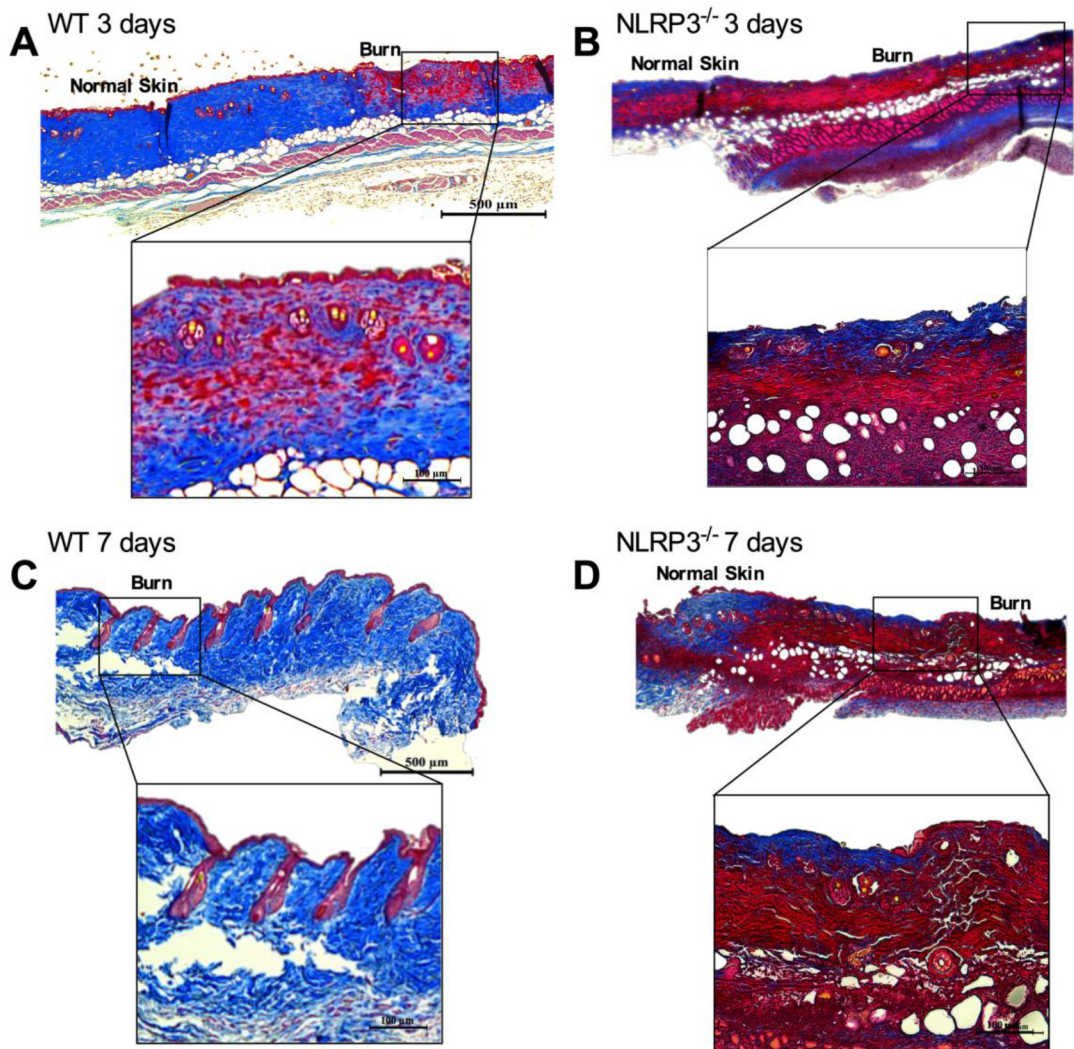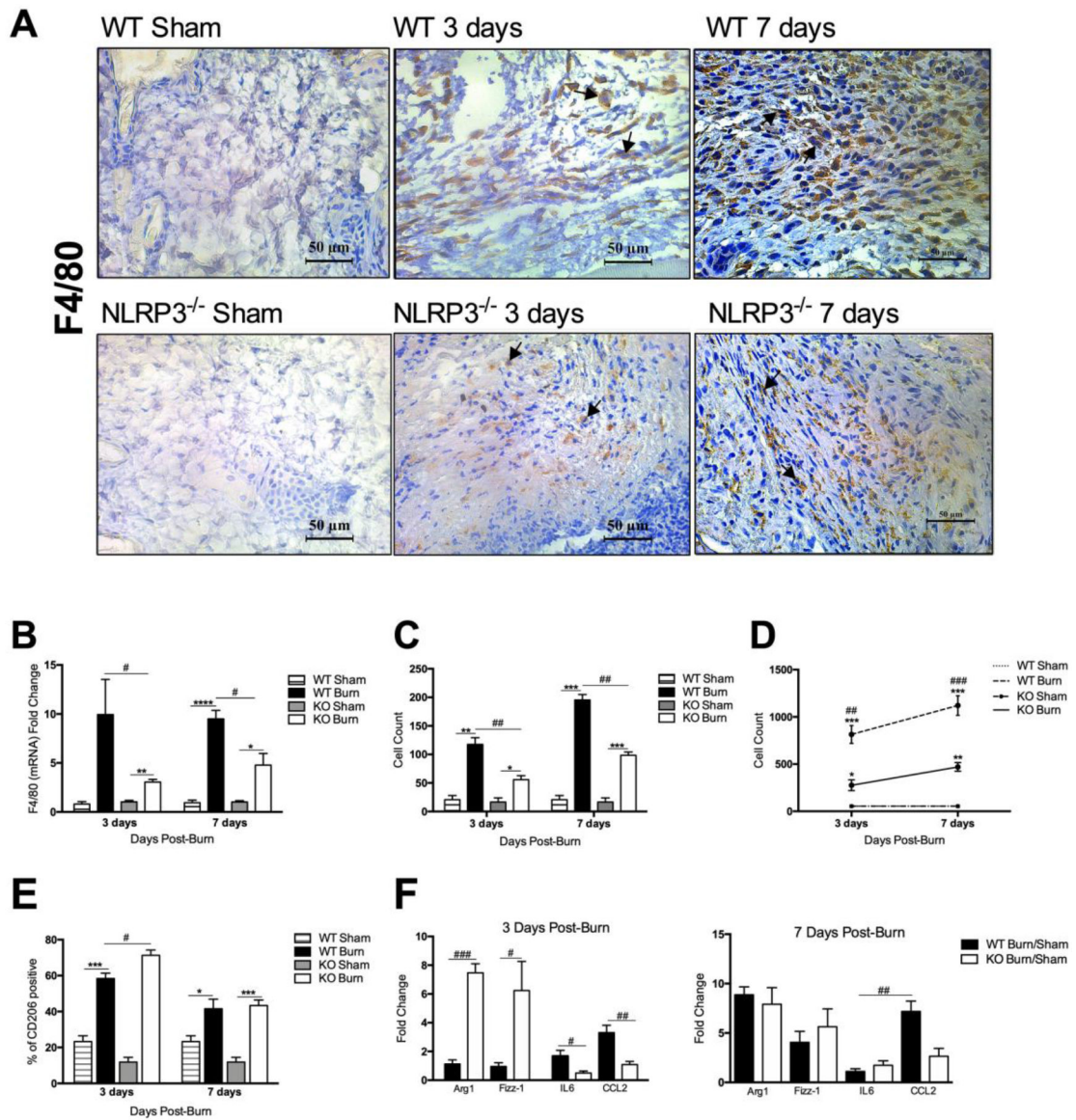
Figure 2.
Impaired wound healing in NLRP3$^{-/-}$. Trichrome staining of excised burn wounds in WT at
(**a**) 3 days and (**c**) 7 days exhibits greater dermal collagen deposition and keratinization
compared to NLRP3$^{-/-}$ at (**b**) 3 days and (**d**) 7 days post-burn. "Normal skin" demarcates
the edge of the wound, and "burn" denotes the wound.

Figure 3.
Reduced macrophage proportion acutely after burn in NLRP3$^{-/-}$. (**a**) F4/80 staining for macrophage infiltration in NLRP3$^{-/-}$ and WT mice shams, 3 days and 7 days after burn is corroborated by (**b**) PCR analysis, which indicates greater expression of F4/80 in WT at both time points. (**c**) F4/80-positive cell counts obtained at 40X magnification (n=3). (**d**) Flow cytometry for skin macrophage distribution shows greater macrophage infiltration in WT. (**e**) Flow cytometry analysis for CD206-positive anti-inflammatory macrophages indicates a greater percentage in NLRP3$^{-/-}$ at 3 days compared to WT. (**f**) Expression of pro- and anti-inflammatory markers at 3 days indicates a pro-inflammatory profile in WT and an anti-inflammatory profile in NLRP3$^{-/-}$, with no significant differences in marker expression between WT and NLRP3$^{-/-}$ at 7 days. Values are presented as mean ± standard error. Burn versus sham *p < 0.05; **p < 0.01; ***p< 0.001, WT versus NLRP3$^{-/-}$ burn #p < 0.05; ##p < 0.01; ###p < 0.001.
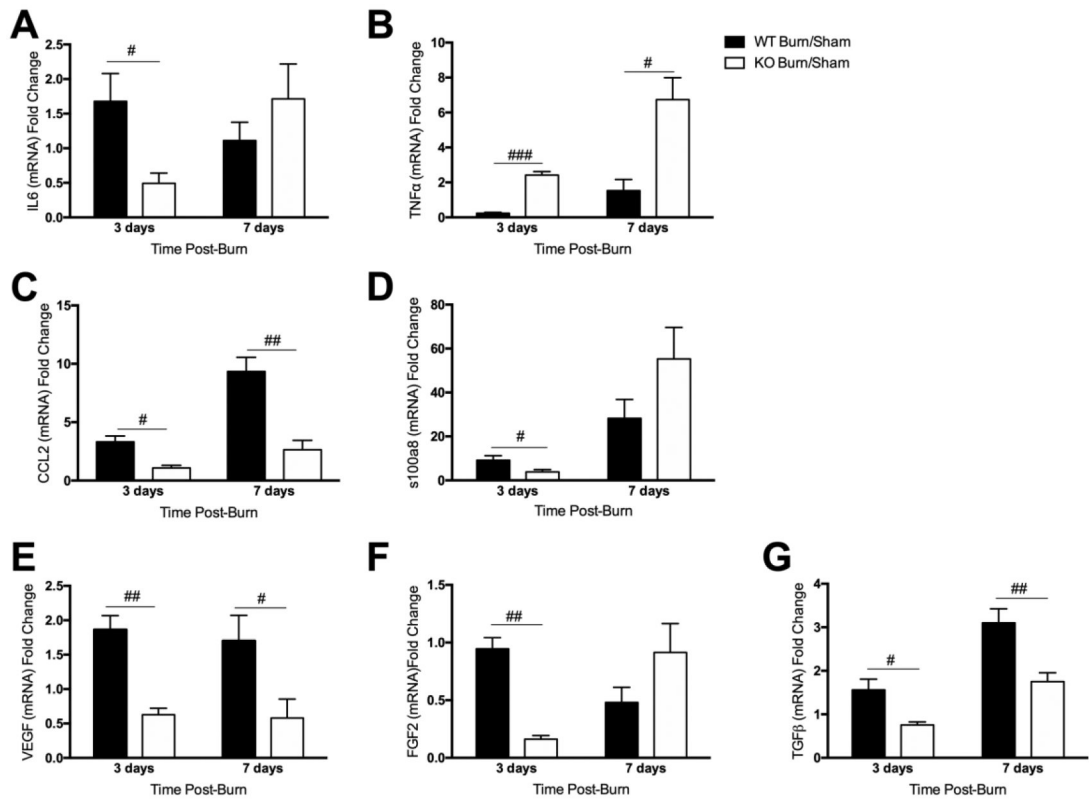
Figure 4.
Decreased expression of pro-inflammatory cytokines, chemokines, and growth factors in NLRP3$^{-/-}$ skin. Gene expression of the inflammatory cytokines (**a**) IL6 and (**b**) TNFα, chemokine (**c**) CCL2, inflammatory mediator (**d**) s100a8, and growth factors (**e**) VEGF, (**f**) FGF2 and (**g**) TGFβ. Values are presented as mean burn/sham ± standard error. WT versus NLRP3$^{-/-}$ burn/sham [#]p < 0.05; [##]p< 0.01; [###]p<0.001.
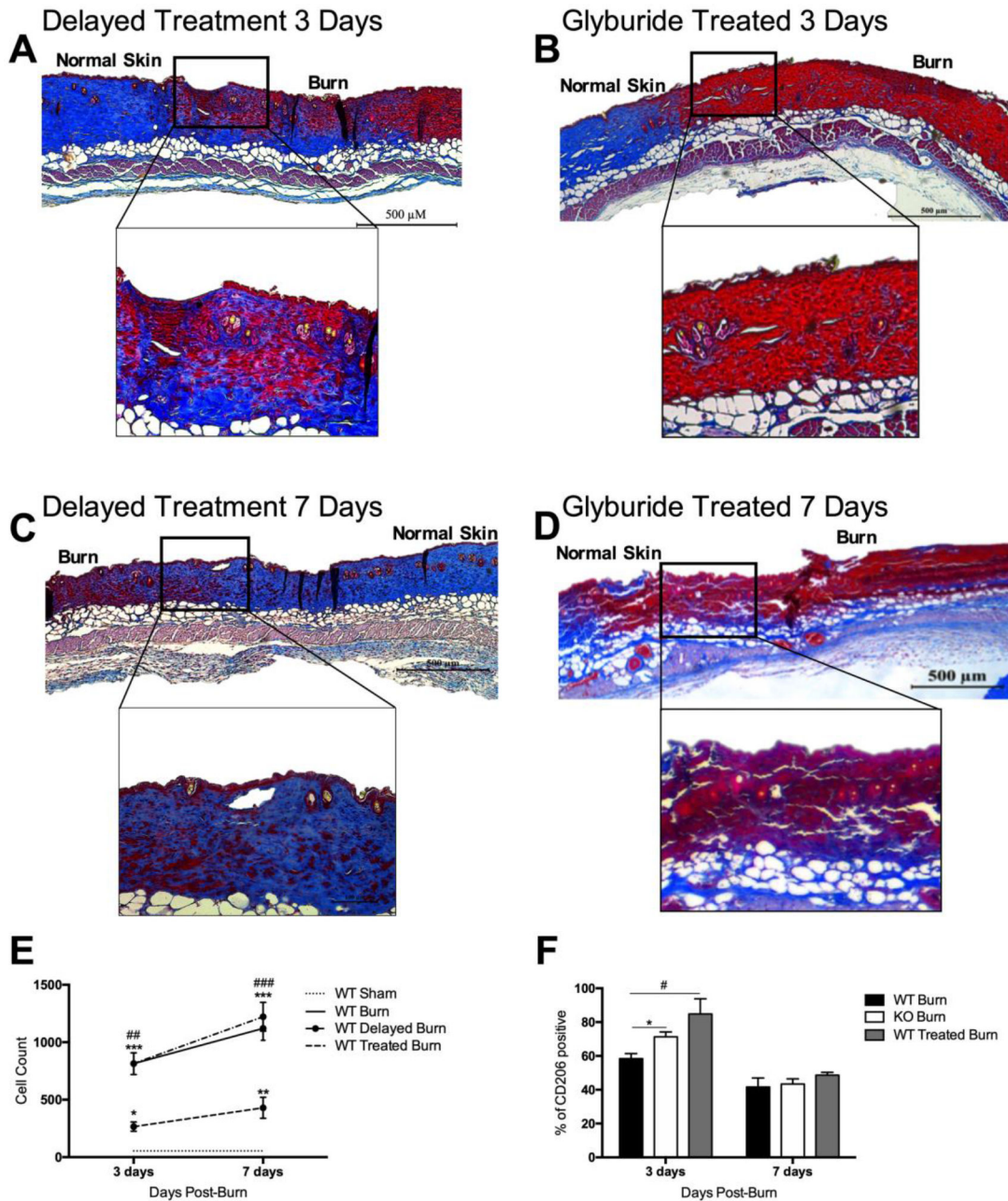
Figure 5.
Inhibition of NLRP3 during the acute phase with glyburide impairs wound healing. Similar to NLRP3$^{-/-}$, trichrome staining of excised burn wounds in treated mice at (**b**) 3 days and (**d**) 7 days exhibit decreased dermal collagen deposition and keratinization compared to delayed treated mice (**a,c**). (**e**) Flow cytometry in glyburide treated skin shows significantly lower levels of macrophages compared to WT and (**f**) greater CD206-positive macrophages at 3 days. "Normal skin" demarcates the edge of the wound, and "burn" denotes the wound. Values are presented as mean burn/sham ± standard error. WT versus NLRP3$^{-/-}$ burn #$p < 0.05$; ##$p < 0.01$; ###$p < 0.001$, WT versus glyburide treated burn *$p < 0.05$; **$p < 0.01$; ***$p < 0.001$.
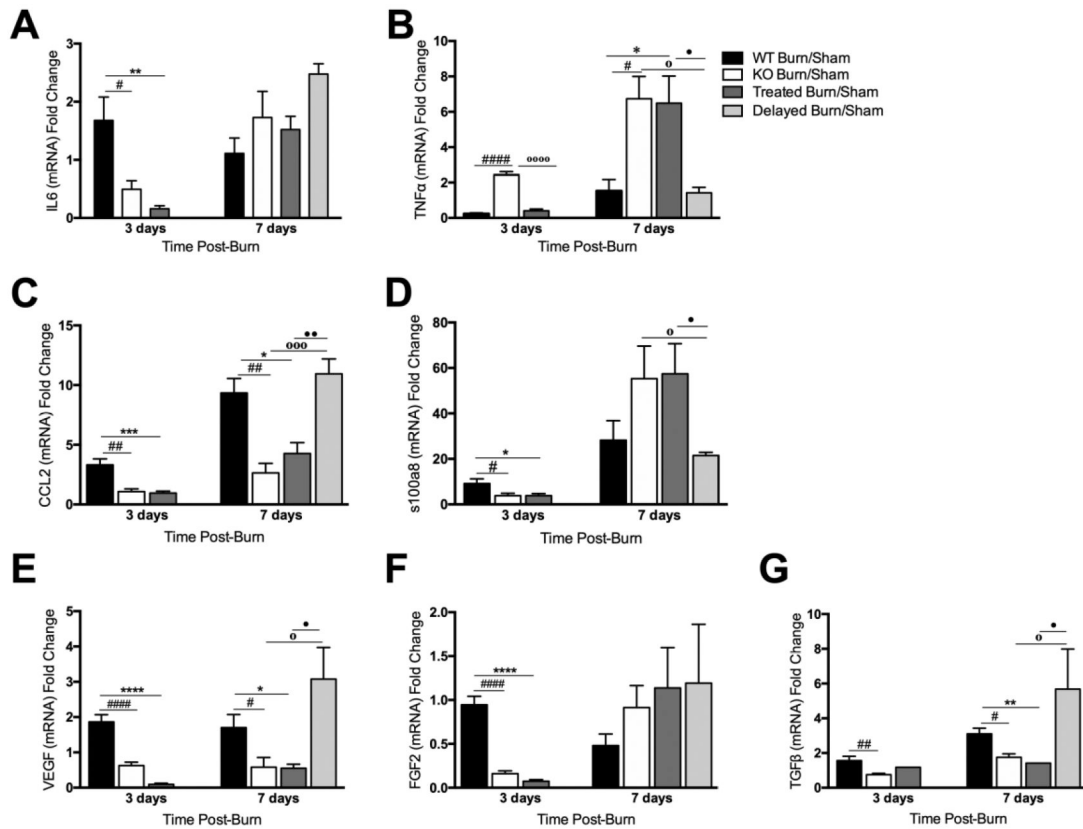
Figure 6.
Glyburide treatment results in comparable reductions in pro-inflammatory cytokines, chemokines, and growth factors to NLRP3$^{-/-}$. Gene expression of the inflammatory cytokines (**a**) IL6 and (**b**) TNFα, chemokine (**c**) CCL2, inflammatory mediator (**d**) s100a8, and growth factors (**e**) VEGF, (**f**) FGF2 and (**g**) TGFβ. Values are presented as mean ± standard error. WT versus NLRP3$^{-/-}$ burn $^{\#}p < 0.05$; $^{\#\#}p < 0.01$; $^{\#\#\#}p < 0.001$, WT versus glyburide treated burn $*p < 0.05$; $**p < 0.01$; $***p < 0.001$, NLRP3$^{-/-}$ versus glyburide treated burn $^{\circ}p < 0.05$; $^{\circ\circ}p < 0.01$; $^{\circ\circ\circ}p < 0.001$, daily treated versus delayed treatment $^{\bullet}p < 0.05$; $^{\bullet\bullet}p < 0.01$; $^{\bullet\bullet\bullet}p<0.001$.